

Cite this: *RSC Adv.*, 2017, 7, 23265

Synthesis and biological evaluation of 3-amino-3-hydroxymethyloxindoles as potential anti-cancer agents†

Kaili Jia,‡ Xinxin Lv,‡ Dong Xing, Jiuwei Che, Donglan Liu, Nilesh J. Thumar, Suzhen Dong* and Wenhao Hu *

A series of substituted 3-amino-3-hydroxymethyloxindoles (**4a–4i**) synthesized through a multi-component approach showed anticancer potency *via in vitro* cytotoxicity screening. Further, to develop the efficiency, derivatives (**5a–5m**) were synthesized and evaluated for their anti-proliferation activity. The most potent compound **5m** showed cytotoxic effect toward SJSA-1 cells ($IC_{50} = 3.14 \mu M$) as well as inhibiting the growth of other cancer cell lines (HCT-116, Jurkat, KB and Bel7402). Further investigation revealed that **5m** induced a significant G2/M cell cycle arrest and time- and dose-dependent cellular apoptosis in SJSA-1 cells. These results suggested that new compound **5m** has anti-proliferating and pro-apoptotic effects, which might be a candidate for cancer therapies.

Received 29th November 2016
Accepted 15th April 2017

DOI: 10.1039/c6ra27536b

rsc.li/rsc-advances

Introduction

Although tremendous efforts and resources have been invested for many years in the development of novel anti-cancer therapies, cancer remains the second leading cause of mortality in the world. It has been reported that a total of 1 658 370 new cancer cases and 589 430 cancer deaths are projected to occur in the United States in 2015.¹ New approaches to treat cancers are urgently needed. The paradigm of novel anticancer drug discovery has been shifted to molecularly-targeted therapeutics, but the conventional approach to drug discovery based on identification of cytotoxic agents on multiple human tumor cell lines, one kind of phenotypic screening, remains the single most successful route.²

Compared to target-based screening, phenotypic screening without particular target in drug discovery highly depends on the quality of new molecule entities with molecular complexity and diversity.^{3,4} Fortunately, such screening library of complex and diverse compounds simultaneously with new scaffolds can be quickly and easily built through multi-component reactions (MCRs).⁵ Our group has developed a series of ylides or zwitterionic intermediates “trapping” MCRs which have been verified as an efficient approach to form heterocycle.^{6–10} Rh(II) catalyzed MCR of 3-diazoindoles, anilines and formalin synthesized 3-

amino-3-hydroxymethyloxindoles type scaffolds.¹¹ Further, screening of synthesized compounds has revealed their anti-cancer activity. Inspired by the primary results, we further synthesized a series of oxindole derivatives to evaluate their anti-proliferation activity for advance study. The compounds with the best activity were assessed for wide-spectrum anti-cancer studies and analyzed for its effects on cell cycle and apoptosis.

Results and discussion

Chemistry

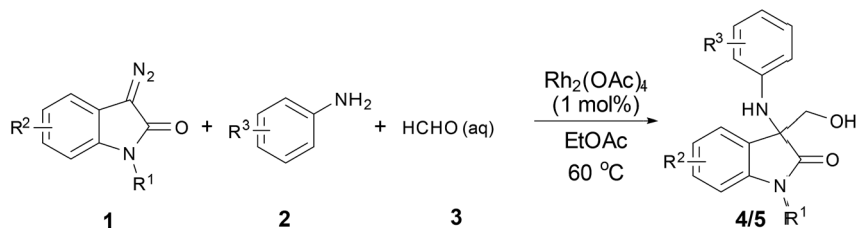
Herein, oxindole derivatives (**4a–4i**, **5a–5m**) were synthesized by three-component “trapping” reaction (Scheme 1) as following: in ethyl acetate (EA) solution of catalyst $Rh_2(OAc)_4$, (1 mol%), aniline **2** and formalin **3** was added sequentially. The suspension was stirred at 60 °C for several minutes. Afterwards, 3-diazoindoles **1** in EA was added to suspension over 1 hour *via* a syringe pump at the same temperature. Upon completion of the addition, the reaction mixture was left on stirring for an additional hour until no further transformation was monitored by TLC test. Solvent was evaporated and the residue was purified by flash chromatography on silica gel to afford the products in moderate yield (53–89%).

As marked in the Scheme 2, the benzyl, methyl and phenyl group which is represented by R^1 , R^2 and R^3 in Table 1 were chemically modified. According to primary biological test results mentioned in Table 1, we realized that the benzyl group at R^1 position and the methyl group at R^2 position were more efficient at respective positions for the antitumor activity of these compound analogues. These results diverted our attention modification at R^3 position. In order to compare the effect

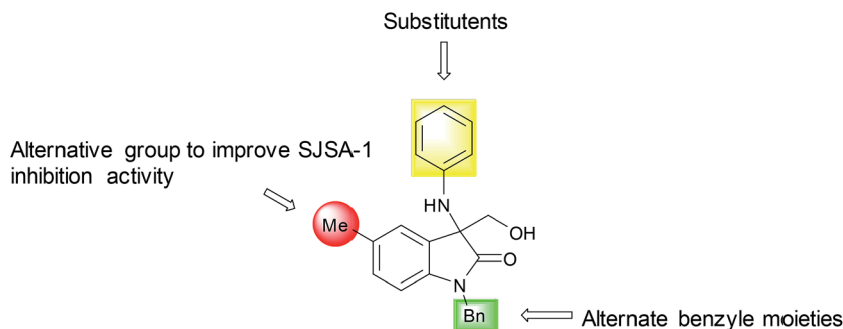
Shanghai Engineering Research Center of Molecular Therapeutics and New Drug Development, School of Chemistry and Molecular Engineering, East China Normal University, 3663 North Zhongshan Road, Shanghai 200062, China. E-mail: szdong@brain.ecnu.edu.cn; whu@chem.ecnu.edu.cn

† Electronic supplementary information (ESI) available. See DOI: 10.1039/c6ra27536b

‡ These authors contribute to this paper equally.



Scheme 1 Synthesis of 3-amino-3-hydroxymethyloxindoles 4 & 5.



Scheme 2 Library optimization strategy for 3-amino-3-hydroxymethyloxindoles to improve SJSA-1 inhibition activity.

on bioactivity of different abundant groups at R³ position, we have prepared a series of analogues having groups such as -F, -Cl, -Br, -I and -NO₂, on the phenyl ring at R³ position and studied subsequently.

Table 1 Inhibitory activity of compounds **4a–4i** and **5a–5m** on SJSA-1 cell proliferation present as inhibition (%) and IC₅₀ (μM)^a

Compound	R ¹	R ²	R ³	Inhibition (%)	IC ₅₀ (μM)
4a	Me	H	2,6-Di-Cl	16.14	— ^b
4b	Bn	H	2,6-Di-Cl	32.69	—
4c	Bn	5-Br	2,6-Di-Cl	90.78	5.74
4d	Bn	H	2,4-Di-Cl	−1.73	—
4e	Bn	H	2-I	41.59	—
4f	Bn	H	4-Cl	89.23	3.5
4g	Bn	H	4-Br	41.46	—
4h	Bn	H	4-I	69.46	2.94
4i	Bn	H	4-NO ₂	97.12	10.81
5a	Bn	H	2-F	7.51	—
5b	Bn	H	3,5-Di-CF ₃	37.90	—
5c	Bn	H	3,4-Di-F	23.66	—
5d	Bn	H	2-Cl-4-F	25.83	—
5e	Bn	H	2,6-Di-F	−4.67	—
5f	Me	H	2,6-Di-F	7.29	—
5g	Me	5-F	2,6-Di-F	19.86	—
5h	Bn	5-Me	2,6-Di-F	38.56	—
5i	4-Me-Bn	H	2,6-Di-F	90.08	6.99
5j	4-Me-Bn	H	2,4-Di-F	81.03	6.19
5k	Bn	H	2,4-Di-F	25.31	—
5l	Bn	5-F	2,4-Di-F	48.41	—
5m	Bn	5-Me	2,4-Di-F	93.65	3.14

^a Inhibition of SJSA cell proliferation produced by the tested compounds at 10 μM. ^b The IC₅₀ of compounds were not determined since the inhibition rate at 10 μM was lower than 50%.

Biological activities

Anti-proliferative activity evaluation. Our random screening had found some of 3-amino-3-hydroxymethyloxindoles had antitumor activity. To obtain new compounds with anticancer activity, CCK-8 assay was used to measure the cytotoxicity of all the known and newly-synthesized substituted 3-amino-3-hydroxymethyloxindoles in SJSA-1 cells. The results are summarized in Table 1. A total of seven compounds had good growth inhibitory activity when used at 10 μM. These compounds were further measured their IC₅₀ values of cytotoxic effects. The IC₅₀ value ranged from 2.94 to 10.81 μM. Among them, compounds **4h** and **5m** showed the most potent inhibitory effects with IC₅₀ values of about 3 μM.

Regarding the structure–activity relationship, several correlations can be made from these data. Compound **4c** with 5-Br substituent on oxindole ring has shown more inhibition activity than **4b**. Through the evaluation of R¹ group, with benzyl (**4b**) moiety replaced by methyl group (**4a**), a previous suppression on the inhibition percentage has been observed. As the affection of R² group was concerned, we attempted to refine the hydrogen (**5e**, **5f**) with fluorine atom (**5g**, **5l**) and methyl group (**5h**, **5m**). We were pleased to find a considering increase on the cytotoxic activity when methyl group (**5h**, **5m**) appears on R¹ position. So, with this optimal condition in hand, we introduced a series of substitute group on R³ phenyl group. After comparison of the bioactivity data, the 2,4-difluorine-phenyl group was considered competent in the R³ position. Another noteworthy point is 4-Cl (**4f**) and 4-I (**4h**) were expelled from preferable list due to its high IC₅₀ value which failed to satisfy our basic requirement even though they show off significantly valuable activity on SJSA-1 inhibition percentage test.



Table 2 *In vitro* cytotoxicity of compound **5m** on five human cancer cell lines and two normal cell lines

Cell	SJSA-1	HCT116	Jurkat	KB	Bel7402	HEK293	HL7702
IC ₅₀ (μM)	3.14	5.1	5.38	18.35	25.04	11.83	39.19

To ensure if these compounds had broad-spectrum anti-cancer activity and preference of killing cancer cells over normal cells, the IC₅₀ of proliferation inhibition was also measured in other four cancer cell lines and two normal cell lines. Compound **5m** also showed some extent of anti-proliferation activities in all the four cells lines (IC₅₀ = 5.1 μM, 5.38 μM, 18.35 μM, 25.04 μM for HCT116, Jurkat, KB, Bel7402 cells, respectively, Table 2). The IC₅₀ of cytotoxicity in HL7702 and HEK293 cells is 39.19 μM and 11.83 μM, respectively. Therefore, **5m** showed better effects of growth inhibition in SJSA-1, HCT116 and Jurkat cells than other cancer and normal cells.

Cell cycle analysis. It is well known that inhibitors of cell proliferation work by interfering with cell cycle or inducing cell death. In order to identify whether compound **5m** has any effects on cell cycle, SJSA-1 cells were treated with compound **5m** at different concentration (0 μM, 2 μM, 5 μM, 10 μM or 20 μM) for 48 h, the cells were collected, stained with PI, and

analyzed their cell cycle distribution by flow cytometry. The results showed that 57.46% of cells were in the G0/G1 phase, 7.56% in the S phase, and 28.22% in the G2/M phase in the control group (Fig. 1A and B). On the contrast, a significant decreased percentage of cells were in G0/G1 phase 48 h following compound **5m** treatment at higher concentration (51.76%, 42.79% and 25.1% for 5 μM, 10 μM and 20 μM, respectively). Meanwhile, the proportion of cells in G2/M phase were significantly increased (30.65%, 35.67% and 44.88% for 5 μM, 10 μM and 20 μM, respectively) (Fig. 1A and B). These results suggested that compound **5m** treatment induced cell cycle arrest at G2/M in a dose-dependent manner, which might be one of the primary mechanisms responsible for the anti-cancer activity of the compound.

Apoptosis induction. In the experiment of cell cycle analysis by flow cytometry, we observed that more and more compound-treated cells entered subG0 phase (3.27%, 7.68% and 15.1% for 5 μM, 10 μM and 20 μM, respectively; compared with control, 0.47%) (Fig. 1), a phrase related to cell apoptosis, which suggested that compound **5m** could also induced cell apoptosis. In order to further confirm the effect, SJSA-1 cells were treated with **5m** at different concentrations (0 μM, 2 μM, 5 μM or 10 μM) and Hoechst 33 342 staining using microscopy were carried out 24 h, 48 h or 72 h after treatment. In the control cells (treated with only the vehicle DMSO), the cells kept growing without visible apoptosis. On the contrast, shrunken nucleus and peripherally clumped and fragmented chromatin were observed following compound treatment at higher concentration (5 μM and 10 μM), a typical characteristic of cells undergoing apoptosis (Fig. 2).

To further quantify the effects of **5m**-induced apoptosis, Annexin V-FITC and PI dual staining were performed using flow cytometry. The analysis of stained cells distinguished between four groups: (1) viable cells (Annexin V⁻, PI⁻); (2) early apoptotic cells (Annexin V⁺, PI⁻); (3) late apoptotic cells (Annexin V⁺, PI⁺); (4) necrotic cells (Annexin V⁻, PI⁺). Firstly, we detected the time-dependent apoptosis. SJSA-1 cells were treated by **5m** at 10 μM

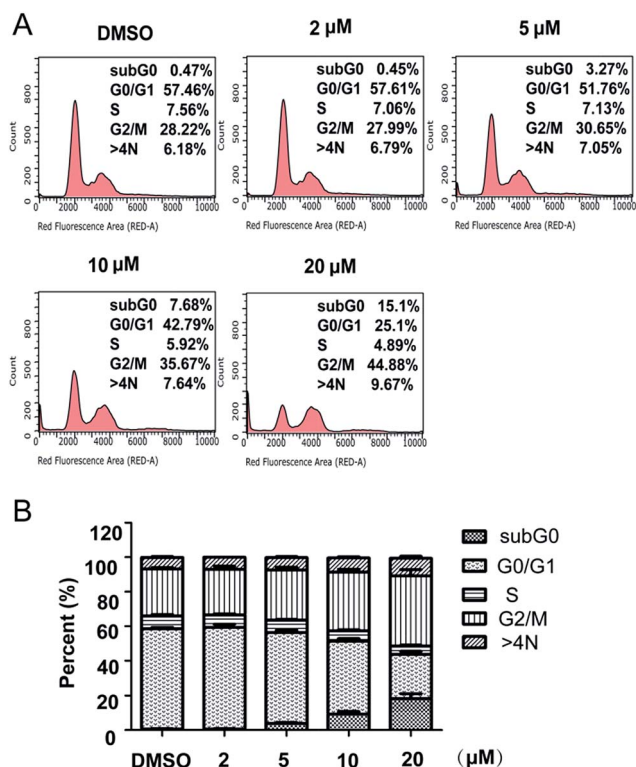


Fig. 1 Effect of compound **5m** on cell cycle progression in SJSA-1 cells. Cells were treated with compound **5m** at 0, 2, 5, 10 or 20 μM for 48 h, stained with PI. Then cell cycle was analyzed by flow cytometry. (A) Representative photographs from three independent experiments were displayed. (B) Cell cycle proportion in (A) was quantitated. Data presented are the mean ± SD of three independent experiments.

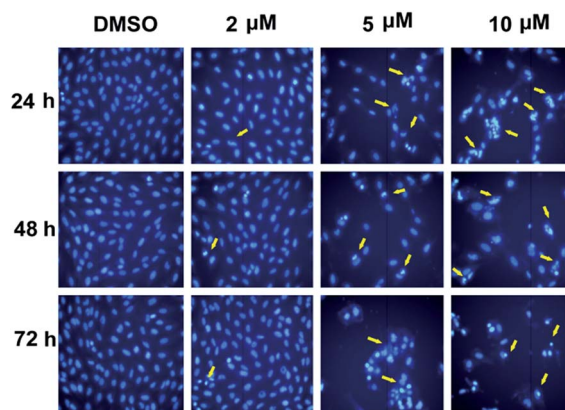


Fig. 2 Compound **5m** induced apparent cell apoptosis. Cells were treated with compound **5m** at 0, 2, 5, or 10 μM for 24 h, 48 h or 72 h and nuclear morphology was checked by Hoechst 33 342 staining by microscopy at 200× and representative photographs were captured. The yellow arrows stand for nucleus of apoptotic cells.



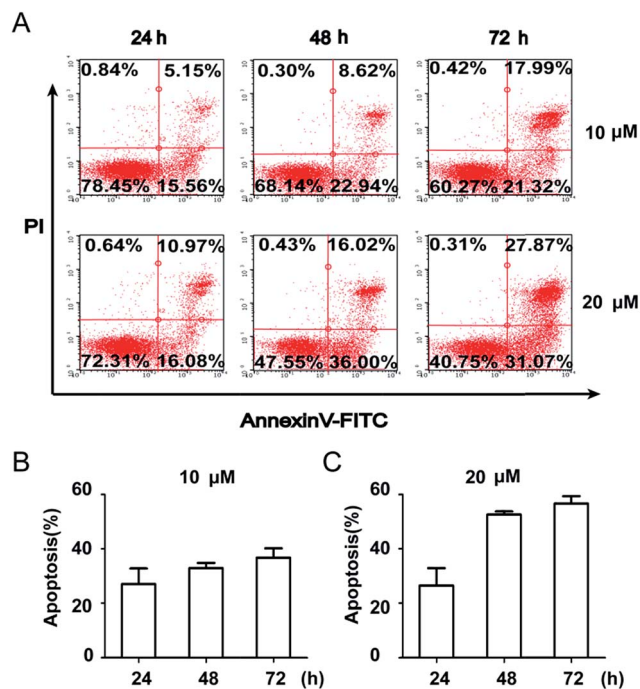


Fig. 3 Time-dependent cellular apoptosis. Cells were treated with compound **5m** at 10 or 20 μM for 24 h, 48 h or 72 h and apoptosis was evaluated using Annexin V-FITC/PI dual staining kit by flow cytometry. (A) Representative photographs from three independent experiments were displayed. (B) Cell apoptosis rates were calculated and plotted in response to different time.

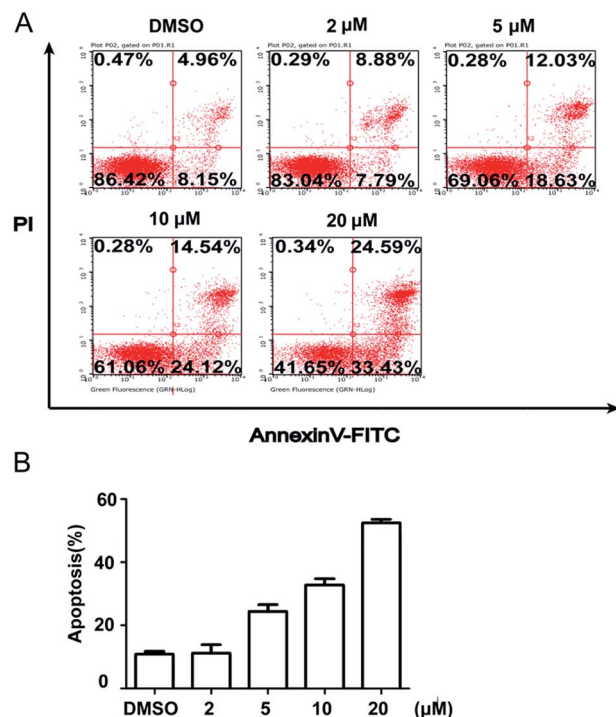


Fig. 4 Concentration-dependent cellular apoptosis. Cells were treated with compound **5m** at 0, 2, 5, 10 or 20 μM for 48 h and apoptosis was evaluated using Annexin V-FITC/PI dual staining kit by flow cytometry. (A) Representative photographs from three independent experiments were displayed. (B) Cell apoptosis rates were calculated and plotted in response to different concentrations.

or 20 μM for 24 h, 48 h or 72 h and then were subject to apoptosis evaluation. The results showed that the percentage of apoptotic cells (including early apoptotic and late apoptotic population) at both concentrations was elevated as the treatment time was extended (Fig. 3). In another experiment, **5m** at different concentration were added into SJSA-1 cells and its effects were analyzed after 48 h. Similarly, **5m** at high concentration induced more apoptotic cells than lower concentration (2 μM , 16.67%; 5 μM , 30.66%; 10 μM , 38.66%; 20 μM , 58.02%) (Fig. 4), suggesting a dose-dependent effect. Therefore, compound **5m** induced apoptosis of SJSA-1 cells in a time- and dose-dependent manner. Moreover, western blotting experiments were performed to study the underlying mechanism of **5m**-induced apoptosis. Our preliminary data (refer ESI†) showed that **5m** caused the ratio of Bax/Bcl-2, two apoptosis-related proteins, to be increased, suggesting that the intrinsic mitochondrial apoptosis pathway, rather than the extrinsic pathway, was involved in **5m**-induced apoptosis. Further investigations are essential to illuminate the accurate mechanism.

Conclusion

In this study, we synthesized a potent series of oxindole compounds (**4a–4i**, **5a–5m**) using MCR approach.¹¹ These compounds were screened for anticancer activity using the CCK-8 assay. Among them, compound **4h** and **5m** displayed the most potent anti-proliferating effect against SJSA-1 cells ($\text{IC}_{50} \approx 3.0 \mu\text{M}$). Besides, **5m** showed broad-spectrum anti-cancer activity because it can inhibit the proliferation of other cancer cells. The flow cytometry results showed that **5m** inhibited the cell growth and caused the cell cycle to be arrested at the G2/M phase. Meanwhile, **5m** induced apoptosis of SJSA-1 cells in a dose- and time-dependent manner. These data proved the potent cell proliferation inhibitory abilities and pro-apoptotic activities of compound **5m** in SJSA-1 cells. To sum up, we regarded compound **5m** as a promising, potent anti-cancer candidate among the 3-amino-3-hydroxymethyloxindoles studied. Further study on the *in vivo* anticancer effects of **5m** compound and its underlying mechanism is in progress.

Materials and methods

Chemicals

Diazocompound **1** was prepared according to the literature methods.^{12–14} All isolated compounds were characterized on the basis of ^1H NMR and ^{13}C NMR spectroscopic data and HRMS (TOF-Q) data. ^1H NMR and ^{13}C NMR chemical shifts are reported in ppm using tetramethylsilane (TMS) as an internal standard.

General procedure for the synthesis of 3-amino-3-hydroxymethyloxindoles (**4a–4i** and **5a–5m**)

To a mixture of $\text{Rh}_2(\text{OAc})_4$ (0.001 mmol), aniline **2** (0.10 mmol), formalin **3** (37% aqueous solution of formaldehyde, 0.60 mmol) in EtOAc (1.0 mL) at 60 $^\circ\text{C}$ and diazo compound **1** (0.1 mmol) in



EtOAc (1.0 mL) were added *via* a syringe pump for 1 h. After the completion of the addition, the reaction mixture was stirred for additional 1 h. Solvents were removed under reduced pressure to give the crude products. The crude products were purified by flash chromatography on silica gel (ethyl acetate/petroleum ether = 1 : 10 to 1 : 1) to give pure products. The compounds (**4a–4i**) were prepared according to literature methods.¹¹

Cell culture

Five human cancer cell lines and two human normal cells were used in the study, including SJSA-1 (osteosarcoma), HCT116 (colon cancer), Bel7402 (liver cancer), KB (Oral epithelial carcinoma), Jurkat (human T lymphocyte leukaemia), HL7702 (normal liver) and HEK293 cells (embryonic kidney). They were purchased from Cell Bank of China Science Academy (Shanghai, China), and cultured aseptically using the corresponding media supplemented with 10% (v/v) fetal bovine serum and 100 units per mL each of penicillin and streptomycin, pH 7.2 and 5% CO₂ humidified atmosphere at 37 °C.

Cell viability assay (cck-8 assay)

In vitro cytotoxicity of the compounds was evaluated by the CCK-8 assay. Briefly, SJSA-1 cells were respectively trypsinized and seeded in 96-well plates at a proper density the day before compound administration. Each tested compound was dissolved in DMSO (10 mM) and diluted in media. Then the compound was added to the cells at 10 µM. The control cells were treated with the vehicle DMSO. After 72 h incubation, 10 µL of CCK8 solution (5 g L⁻¹; Yeasen) in the media was added to each well and incubated for additional 4 h. Finally, the optical density (OD) was measured at 450 nm using a microplate reader (spectraMax M5/M5e, Sunnyvale, CA, USA) and a reference wavelength at 620 nm. If one compound inhibits cell proliferation with percentage inhibition higher than 50%, the IC₅₀ value was determined by testing the inhibitory effects of the compound with 10 gradient-dilution concentrations with at least three replicates per concentration. As for the compound with the best growth-inhibitory activity, its IC₅₀ value in other six cell lines (HCT116, Bel7402, KB, Jurkat, HL7702 and HEK293) were further determined.

Cell cycle analysis

Cell cycle analysis was performed to check the distribution of SJSA-1 cells in different phases caused by compound **5m** using propidium iodide (PI) staining method. SJSA-1 cells were plated in 6-well plates (1 × 10⁵ cells per well), and allowed to grow to about 70% to 80% confluence and then the cells were exposed to compound **5m** at a concentration of 0, 2, 5, 10 or 20 µM, respectively. After 48 h, cells were trypsinized, washed with cold PBS, and permeabilized with 70% ethanol overnight. On the next day, the cells were stained with PI (Beyotime) according to the manufacturer's instructions. Then cells were measured using an easyCyte 6HT-2L (Millipore) and analyzed by FlowJo software. All experiments were conducted in triplicate, and for each measurement, at least 20 000 cells were counted.

Hoechst staining

Nuclear morphology was detected by staining nuclei with Hoechst 33 342. SJSA-1 cells (1 × 10⁴) were seeded in twenty-four-well plates for 24 h. Thereafter, cells were treated with compound **5m** at different concentration for 24 h, 48 h or 72 h. Cells were washed with PBS and fixed with 4% paraformaldehyde. Cells were stained with Hoechst 33 342 and images were captured using fluorescence microscope (Leica).

Annexin V-FITC/PI dual staining

To determine effect of compound **5m** on apoptosis in SJSA-1 cells, Annexin V-FITC/PI dual staining was carried out by flow cytometry. SJSA-1 cells (1 × 10⁵ cells per well) were seeded in six-well plates and allowed to grow to 70 to 80% confluence. Then the cells were treated with compound **5m** at concentrations of 0, 2, 5, 10 or 20 µM for 48 h, respectively (dose-response experiment) or 10 µM and 20 µM for 24 h, 48 h or 72 h, respectively (time-response experiment). At the end of the incubation, the cells were harvested by trypsinization and washed twice with cold PBS. Then the cells were resuspended in 400 µL of 1× binding buffer and stained with Annexin V-FITC and PI using the apoptosis detection kit from Beyotime. Cells were measured using an easyCyte 6HT-2L (Millipore) and analyzed by FlowJo software. The percentage of cells for the lower and upper right quadrant was used for statistical analysis using Graphpad Prism 5. All experiments were conducted in triplicate, and for each measurement, at least 1 × 10⁴ cells were counted.

1-Benzyl-3-((2-fluorophenyl)amino)-3-(hydroxymethyl)indolin-2-one (5a). A white solid (73% yield). ¹H NMR (400 MHz, CDCl₃) δ 7.30 (qd, *J* = 6.6, 3.3 Hz, 7H), 7.08 (t, *J* = 7.5 Hz, 1H), 6.96 (ddd, *J* = 11.6, 8.0, 1.4 Hz, 1H), 6.88 (d, *J* = 7.8 Hz, 1H), 6.65–6.58 (m, 1H), 6.53 (t, *J* = 7.6 Hz, 1H), 5.78–5.71 (m, 1H), 5.47 (d, *J* = 3.2 Hz, 1H), 5.12 (d, *J* = 15.4 Hz, 1H), 4.80 (d, *J* = 15.4 Hz, 1H), 3.97 (t, *J* = 11.4 Hz, 1H), 3.73 (dd, *J* = 11.5, 2.5 Hz, 1H), 2.91 (dd, *J* = 11.3, 2.6 Hz, 1H). ¹³C NMR (100 MHz, CDCl₃) δ 177.58, 153.55, 151.17, 141.86, 135.32, 134.03 (d, *J* = 11.2 Hz), 129.77, 128.87, 127.98, 127.72, 127.25, 124.23 (d, *J* = 3.7 Hz), 124.03, 123.64, 118.96 (d, *J* = 7.2 Hz), 114.91, 114.73, 114.30 (d, *J* = 2.4 Hz), 110.11, 99.99, 68.07, 64.38, 44.18. HRMS (ESI) calcd for C₂₂H₁₉FN₂O₂ [M + Na]⁺: 385.1328, found 385.1320.

1-Benzyl-3-((3,5-bis(trifluoromethyl)phenyl)amino)-3-(hydroxymethyl)indolin-2-one (5b). A white solid (85% yield). ¹H NMR (400 MHz, CDCl₃) δ 7.38–7.26 (m, 7H), 7.12 (dd, *J* = 14.3, 6.4 Hz, 2H), 6.91 (d, *J* = 7.8 Hz, 1H), 6.61 (s, 2H), 5.63 (s, 1H), 5.06–4.88 (m, 2H), 3.95 (t, *J* = 11.6 Hz, 1H), 3.75 (dd, *J* = 11.6, 1.8 Hz, 1H), 2.90 (dd, *J* = 11.1, 1.8 Hz, 1H). ¹³C NMR (100 MHz, CDCl₃) δ 176.90, 146.36, 141.92, 134.95, 132.34 (d, *J* = 32.9 Hz), 130.40, 129.06, 128.03, 127.15, 125.60, 124.52, 123.94 (d, *J* = 8.6 Hz), 121.81, 114.03 (q, *J* = 3.8, 2.3 Hz), 112.26, 110.51, 67.95, 64.27, 44.36. HRMS (ESI) calcd for C₂₄H₁₈F₆N₂O₂ [M + Na]⁺: 503.1170, found 503.1163.

1-Benzyl-3-((3,4-difluorophenyl)amino)-3-(hydroxymethyl)indolin-2-one (5c). A white solid (67% yield). ¹H NMR (400 MHz, CDCl₃) δ 7.40–7.27 (m, 5H), 7.21 (d, *J* = 7.0 Hz, 2H), 7.10 (t, *J* = 7.4 Hz, 1H), 6.86 (d, *J* = 7.8 Hz, 1H), 6.74 (dd, *J* = 18.6, 9.2 Hz, 1H), 6.13–5.93 (m, 2H), 5.12 (d, *J* = 15.2 Hz, 2H), 4.75 (d, *J* =



15.4 Hz, 1H), 3.91 (t, J = 11.4 Hz, 1H), 3.69 (d, J = 11.3 Hz, 1H), 2.94 (d, J = 11.1 Hz, 1H). ^{13}C NMR (100 MHz, CDCl_3) δ 177.51, 142.46 (dd, J = 8.2, 2.0 Hz), 141.90, 135.12, 129.97, 128.93, 128.02, 127.45, 126.87, 123.86 (d, J = 24.2 Hz), 117.35 (d, J = 18.5 Hz), 111.31 (dd, J = 5.6, 3.3 Hz), 110.30, 104.74 (d, J = 20.6 Hz), 67.88, 65.13, 44.13. HRMS (ESI) calcd for $\text{C}_{22}\text{H}_{18}\text{F}_2\text{N}_2\text{O}_2$ [$\text{M} + \text{Na}$] $^+$: 403.1234, found 403.1233.

1-Benzyl-3-((2-chloro-4-fluorophenyl)amino)-3-(hydroxymethyl)-indolin-2-one (5d). A white solid (53% yield). ^1H NMR (400 MHz, CDCl_3) δ 7.37–7.27 (m, 7H), 7.09 (t, J = 7.5 Hz, 1H), 7.03 (dd, J = 8.2, 2.5 Hz, 1H), 6.91 (d, J = 7.7 Hz, 1H), 6.37 (td, J = 8.6, 2.6 Hz, 1H), 5.72 (s, 1H), 5.64 (dd, J = 8.9, 5.1 Hz, 1H), 5.13 (d, J = 15.3 Hz, 1H), 4.77 (d, J = 15.3 Hz, 1H), 3.98 (t, J = 11.4 Hz, 1H), 3.73 (dd, J = 11.5, 1.7 Hz, 1H), 2.88 (dd, J = 11.3, 1.8 Hz, 1H). ^{13}C NMR (100 MHz, CDCl_3) δ 177.27, 141.82, 138.47 (d, J = 2.5 Hz), 135.29, 129.90, 128.89, 128.10, 127.80, 126.94, 123.98, 123.75, 116.76 (d, J = 25.7 Hz), 113.93 (dd, J = 20.8, 14.9 Hz), 110.16, 68.05, 64.78, 44.20. HRMS (ESI) calcd for $\text{C}_{22}\text{H}_{18}\text{ClFN}_2\text{O}_2$ [$\text{M} + \text{Na}$] $^+$ = 419.0939, found 419.0919.

1-Benzyl-3-((2,6-difluorophenyl)amino)-3-(hydroxymethyl)-indolin-2-one (5e). A white solid (77% yield). ^1H NMR (400 MHz, CDCl_3) δ 7.30 (dd, J = 12.0, 4.8 Hz, 3H), 7.25–7.12 (m, 4H), 6.97 (t, J = 7.5 Hz, 1H), 6.82–6.57 (m, 4H), 5.02–4.82 (m, 3H), 3.95–3.82 (m, 2H), 2.82 (dd, J = 9.5, 4.0 Hz, 1H). ^{13}C NMR (100 MHz, CDCl_3) δ 177.34, 154.81 (dd, J = 242.9, 6.7 Hz), 142.62, 135.56, 129.36, 128.77, 127.70, 127.59, 127.31, 123.74, 122.75, 120.58 (t, J = 9.5 Hz), 111.28 (dd, J = 17.2, 7.0 Hz), 109.58, 68.35, 65.92, 44.04. HRMS (ESI) calcd for $\text{C}_{22}\text{H}_{18}\text{F}_2\text{N}_2\text{O}_2$ [$\text{M} + \text{Na}$] $^+$ = 403.1234, found 403.1224.

3-((2,6-Difluorophenyl)amino)-3-(hydroxymethyl)-1-methyl-indolin-2-one (5f). A white solid (89% yield). ^1H NMR (400 MHz, CDCl_3) δ 7.41 (t, J = 7.7 Hz, 1H), 7.33 (d, J = 7.3 Hz, 1H), 7.14 (t, J = 7.5 Hz, 1H), 6.97 (d, J = 7.8 Hz, 1H), 6.75 (ddd, J = 11.2, 8.5, 2.8 Hz, 1H), 6.43–6.33 (m, 1H), 5.73 (td, J = 9.3, 5.4 Hz, 1H), 5.30 (s, 1H), 5.27 (d, J = 1.8 Hz, 1H), 3.92 (t, J = 11.3 Hz, 1H), 3.68 (dd, J = 11.5, 2.5 Hz, 1H), 3.28 (s, 3H), 2.82 (dd, J = 11.2, 2.5 Hz, 1H). ^{13}C NMR (100 MHz, CDCl_3) δ 177.31, 156.80, 142.77, 130.57, 130.00, 127.12, 124.00, 123.70, 114.29 (dd, J = 8.9, 3.6 Hz), 110.49 (dd, J = 21.8, 3.9 Hz), 109.08, 103.76 (dd, J = 26.6, 23.3 Hz), 67.84, 64.65, 53.50, 26.46. HRMS (ESI) calcd for $\text{C}_{16}\text{H}_{14}\text{F}_2\text{N}_2\text{O}_2$ [$\text{M} + \text{Na}$] $^+$ = 327.0921, found 327.0934.

3-((2,6-Difluorophenyl)amino)-5-fluoro-3-(hydroxymethyl)-1-methylindolin-2-one (5g). A white solid (69% yield). ^1H NMR (400 MHz, CDCl_3) δ 7.00 (td, J = 8.9, 2.6 Hz, 1H), 6.92 (dd, J = 7.5, 2.6 Hz, 1H), 6.79 (dd, J = 8.5, 4.0 Hz, 1H), 6.72–6.62 (m, 3H), 4.95 (s, 1H), 3.88–3.75 (m, 2H), 3.22 (s, 3H), 2.93 (dd, J = 8.6, 4.7 Hz, 1H). ^{13}C NMR (100 MHz, CDCl_3) δ 177.13 (d, J = 0.9 Hz), 160.38, 157.98, 155.48 (d, J = 6.8 Hz), 153.07 (d, J = 6.6 Hz), 139.34, 129.85–129.57 (m), 122.06 (t, J = 15.0 Hz), 120.25 (t, J = 9.6 Hz), 115.71, 115.47, 112.06, 111.81, 111.45, 111.38, 111.28, 111.20 (d, J = 1.7 Hz), 109.06 (d, J = 8.0 Hz), 68.02, 66.01, 26.55. HRMS (ESI) calcd for $\text{C}_{16}\text{H}_{13}\text{F}_3\text{N}_2\text{O}_2$ [$\text{M} + \text{Na}$] $^+$ = 345.0827, found 345.0817.

1-Benzyl-3-((2,6-difluorophenyl)amino)-3-(hydroxymethyl)-5-methylindolin-2-one (5h). A white solid (75% yield). ^1H NMR (400 MHz, CDCl_3) δ 7.32–7.27 (m, 2H), 7.26–7.19 (m, 3H), 7.05–6.94 (m, 2H), 6.80–6.64 (m, 3H), 6.62 (d, J = 7.9 Hz, 1H), 5.01–4.80 (m, 3H), 3.93–3.79 (m, 2H), 2.86 (dd, J = 9.9, 3.7 Hz, 1H), 2.24 (s,

3H). ^{13}C NMR (100 MHz, CDCl_3) δ 177.23, 155.91 (d, J = 6.7 Hz), 153.50 (d, J = 6.7 Hz), 140.14, 135.66, 132.44, 129.59, 128.73, 127.79, 127.64, 127.30, 124.46, 122.40 (t, J = 15.3 Hz), 120.39 (t, J = 9.5 Hz), 111.30 (dd, J = 17.1, 7.0 Hz), 109.32, 68.40, 65.88, 44.04, 21.01. HRMS (ESI) calcd for $\text{C}_{23}\text{H}_{20}\text{F}_2\text{N}_2\text{O}_2$ [$\text{M} + \text{Na}$] $^+$ = 417.1391, found 417.1376.

3-((2,6-Difluorophenyl)amino)-3-(hydroxymethyl)-1-(4-methylbenzyl)indolin-2-one (5i). A white solid (67% yield). ^1H NMR (400 MHz, CDCl_3) δ 7.32 (dd, J = 15.1, 7.6 Hz, 2H), 7.18–7.04 (m, 5H), 6.88 (d, J = 7.8 Hz, 1H), 6.77 (ddd, J = 11.1, 8.6, 2.7 Hz, 1H), 6.28 (t, J = 8.5 Hz, 1H), 5.70 (td, J = 9.3, 5.5 Hz, 1H), 5.32 (d, J = 2.8 Hz, 1H), 5.09 (d, J = 15.3 Hz, 1H), 4.70 (d, J = 15.3 Hz, 1H), 3.96 (t, J = 11.5 Hz, 1H), 3.72 (dd, J = 11.5, 2.2 Hz, 1H), 2.90 (dd, J = 11.4, 2.2 Hz, 1H), 2.33 (s, 3H). ^{13}C NMR (100 MHz, CDCl_3) δ 177.47, 141.92, 137.82, 132.17, 130.46 (dd, J = 11.5, 2.6 Hz), 129.88, 129.52, 127.67, 127.13, 124.05, 123.64, 115.10 (dd, J = 8.8, 3.5 Hz), 110.41 (dd, J = 21.9, 3.8 Hz), 110.23, 103.80 (dd, J = 26.5, 23.5 Hz), 67.86, 64.80, 43.89, 21.14. HRMS (ESI) calcd for $\text{C}_{22}\text{H}_{20}\text{F}_2\text{N}_2\text{O}_2$ [$\text{M} + \text{Na}$] $^+$ = 417.1391, found 417.1385.

3-((2,4-Difluorophenyl)amino)-3-(hydroxymethyl)-1-(4-methylbenzyl)indolin-2-one (5j). A white solid (83% yield). ^1H NMR (400 MHz, CDCl_3) δ 7.31 (dd, J = 15.6, 7.2 Hz, 2H), 7.21–6.98 (m, 5H), 6.88 (d, J = 7.8 Hz, 1H), 6.76 (ddd, J = 11.2, 8.5, 2.8 Hz, 1H), 6.28 (ddd, J = 10.6, 3.2, 1.9 Hz, 1H), 5.71 (td, J = 9.3, 5.5 Hz, 1H), 5.31 (d, J = 2.1 Hz, 1H), 5.08 (d, J = 15.3 Hz, 1H), 4.70 (d, J = 15.3 Hz, 1H), 3.96 (t, J = 11.4 Hz, 1H), 3.72 (dd, J = 11.5, 2.4 Hz, 1H), 2.89 (dd, J = 11.3, 2.4 Hz, 1H), 2.33 (s, 3H). ^{13}C NMR (100 MHz, CDCl_3) δ 177.45, 141.97, 137.81, 132.18, 130.46 (dd, J = 11.3, 4.1 Hz), 129.96, 129.81, 129.64, 129.39, 127.78, 127.53, 127.14, 124.11, 123.97, 123.75, 123.51, 110.22 (d, J = 32.0 Hz), 64.77, 43.90 (dd, J = 20.6, 13.2 Hz), 21.12 (d, J = 18.8 Hz). HRMS (ESI) calcd for $\text{C}_{23}\text{H}_{20}\text{F}_2\text{N}_2\text{O}_2$ [$\text{M} + \text{Na}$] $^+$ = 417.1391, found 417.1382.

1-Benzyl-3-((2,4-difluorophenyl)amino)-3-(hydroxymethyl)-indolin-2-one (5k). A white solid (53% yield). ^1H NMR (400 MHz, CDCl_3) δ 7.39–7.27 (m, 5H), 7.24–7.17 (m, 2H), 7.10 (t, J = 7.5 Hz, 1H), 6.87 (d, J = 7.8 Hz, 1H), 6.82–6.70 (m, 1H), 6.27 (t, J = 8.4 Hz, 1H), 5.72 (td, J = 9.2, 5.8 Hz, 1H), 5.31 (s, 1H), 5.11 (d, J = 15.4 Hz, 1H), 4.75 (d, J = 15.4 Hz, 1H), 3.97 (t, J = 11.4 Hz, 1H), 3.74 (d, J = 11.5 Hz, 1H), 2.89 (d, J = 11.1 Hz, 1H). ^{13}C NMR (100 MHz, CDCl_3) δ 177.48, 141.95, 135.24, 130.42 (dd, J = 11.6, 3.2 Hz), 129.89, 128.86, 128.03, 127.66, 127.18, 124.11, 123.68, 115.31 (dd, J = 8.8, 3.5 Hz), 110.41 (dd, J = 21.6, 3.9 Hz), 110.14, 103.80 (dd, J = 26.5, 23.4 Hz), 67.91, 64.87, 44.12. HRMS (ESI) calcd for $\text{C}_{22}\text{H}_{18}\text{F}_2\text{N}_2\text{O}_2$ [$\text{M} + \text{Na}$] $^+$ = 403.1234, found 403.1222.

1-Benzyl-3-((2,4-difluorophenyl)amino)-5-fluoro-3-(hydroxymethyl)indolin-2-one (5l). A white solid (86% yield). ^1H NMR (400 MHz, CDCl_3) δ 7.35–7.27 (m, 3H), 7.24–7.16 (m, 2H), 7.10 (dd, J = 7.4, 2.5 Hz, 1H), 6.98 (td, J = 8.8, 2.6 Hz, 1H), 6.85–6.71 (m, 2H), 6.36–6.26 (m, 1H), 5.72 (td, J = 9.2, 5.4 Hz, 1H), 5.28 (s, 1H), 5.11 (d, J = 15.4 Hz, 1H), 4.73 (d, J = 15.4 Hz, 1H), 3.94 (t, J = 11.3 Hz, 1H), 3.75 (dd, J = 11.4, 2.4 Hz, 1H), 2.88 (dd, J = 11.1, 2.4 Hz, 1H). ^{13}C NMR (100 MHz, CDCl_3) δ 177.20, 137.77, 134.91, 129.09, 129.02 (d, J = 1.0 Hz), 128.94 (d, J = 3.0 Hz), 128.88, 128.26, 127.75, 127.54, 115.39 (d, J = 3.5 Hz), 115.18, 112.59 (d, J = 6.7 Hz), 112.34, 112.06, 111.07, 110.72 (dd, J = 5.0, 1.9 Hz), 104.14 (d, J = 2.0 Hz), 65.15 (d, J = 1.8 Hz), 44.31, 17.99. HRMS (ESI) calcd for $\text{C}_{22}\text{H}_{17}\text{F}_3\text{N}_2\text{O}_2$ [$\text{M} + \text{Na}$] $^+$ = 421.1140, found 421.1142.



1-Benzyl-3-((2,4-difluorophenyl)amino)-3-(hydroxymethyl)-5-methylindolin-2-one (5m). A white solid (75% yield). ^1H NMR (400 MHz, CDCl_3) δ 7.35–7.26 (m, 3H), 7.22 (dd, $J = 7.0, 2.3$ Hz, 2H), 7.15 (s, 1H), 7.08 (d, $J = 8.0$ Hz, 1H), 6.83–6.68 (m, 2H), 6.38–6.19 (m, 1H), 5.72 (td, $J = 9.3, 5.5$ Hz, 1H), 5.30 (d, $J = 6.6$ Hz, 1H), 5.09 (d, $J = 15.4$ Hz, 1H), 4.72 (d, $J = 15.4$ Hz, 1H), 4.72 (d, $J = 15.4$ Hz, 1H), 3.95 (t, $J = 11.4$ Hz, 1H), 3.71 (dd, $J = 11.5, 1.8$ Hz, 1H), 2.96 (d, $J = 11.3$ Hz, 1H), 2.29 (s, 3H). ^{13}C NMR (100 MHz, CDCl_3) δ 177.39, 156.78 (d, $J = 11.1$ Hz), 154.40 (d, $J = 11.0$ Hz), 153.31 (d, $J = 11.6$ Hz), 150.89 (d, $J = 11.7$ Hz), 139.47, 135.36, 133.48, 130.54 (dd, $J = 11.5, 3.2$ Hz), 130.19, 128.82, 127.98, 127.70, 127.13, 115.08 (dd, $J = 8.8, 3.6$ Hz), 110.41 (dd, $J = 21.7, 3.9$ Hz), 109.94, 103.77 (dd, $J = 26.6, 23.4$ Hz), 67.93, 64.76, 44.14, 21.05. HRMS (ESI) calcd for $\text{C}_{23}\text{H}_{20}\text{F}_2\text{N}_2\text{O}_2$ $[\text{M} + \text{Na}]^+ = 417.1391$, found 417.1389.

Acknowledgements

We wish to thank the Natural Science Foundation of Shanghai (16ZR1410500) for financial support.

Notes and references

- R. L. Siegel, K. D. Miller and A. Jemal, *Ca-Cancer J. Clin.*, 2015, **65**, 5–29.
- A. S. Narang and D. D. Desai, in *Pharmaceutical Perspectives of Cancer Therapeutics*, ed. Y. Lu and R. I. Mahato, 2009, pp. 49–92.
- S. L. Schreiber, *Science*, 2000, **287**, 1964–1969.
- E. Ruijter, R. Scheffelaar and R. V. Orru, *Angew. Chem., Int. Ed.*, 2011, **50**, 6234–6246.
- Y. Xia, Y. Zhang and J. Wang, *ACS Catal.*, 2013, **3**, 2586–2598.
- X. Guo and W. Hu, *Acc. Chem. Res.*, 2013, **46**, 2427–2440.
- D. Xing and W. Hu, *Tetrahedron Lett.*, 2014, **55**, 777–783.
- W. Hu, X. Xu, J. Zhou, W. J. Liu, H. Huang, J. Hu, L. Yang and L. Z. Gong, *J. Am. Chem. Soc.*, 2008, **130**, 7782–7783.
- J. Jiang, H. D. Xu, J. B. Xi, B. Y. Ren, F. P. Lv, X. Guo, L. Q. Jiang, Z. Y. Zhang and W. H. Hu, *J. Am. Chem. Soc.*, 2011, **133**, 8428–8431.
- H. Qiu, M. Li, L. Q. Jiang, F. P. Lv, L. Zan, C. W. Zhai, M. P. Doyle and W. H. Hu, *Nat. Chem.*, 2012, **4**, 733–738.
- C. Wang, D. Xing, D. Wang, X. Wu and W. Hu, *J. Org. Chem.*, 2014, **79**, 3908–3916.
- C. Marti and E. M. Carreira, *J. Am. Chem. Soc.*, 2005, **127**, 11505–11515.
- S. Muthusamy, C. Gunanathan and M. Nethaji, *J. Org. Chem.*, 2004, **69**, 5631–5637.
- M. P. Cava and D. R. Napier, *J. Am. Chem. Soc.*, 1957, **79**, 1701–1705.

